A. H. Nayfeh
C. Chin
D. T. Mook
Department of Engineering Science and Mechanics
Virginia Polytechnic Institute and State University
Blacksburg, VA 24061-0219

Parametrically Excited Nonlinear Two-Degree-of-Freedom Systems with Repeated Natural Frequencies

The method of normal forms is used to study the nonlinear response of two-degree-of-freedom systems with repeated natural frequencies and cubic nonlinearity to a principal parametric excitation. The linear part of the system has a nonsemisimple one-to-one resonance. The character of the stability and various types of bifurcation including the formation of a homoclinic orbit are analyzed. The results are applied to the flutter of a simply supported panel in a supersonic airstream. © *1995 John Wiley & Sons, Inc.*

INTRODUCTION

Parametrically excited two-degree-of-freedom (2-DOF) systems with a nonsemisimple one-to-one resonance are analyzed by the method of normal forms. A system with repeated frequencies is said to have a nonsemisimple one-to-one resonance if its linearized part cannot be diagonalized. The nonlinearity is cubic and the excitation is harmonic. Principal parametric resonance is investigated. The results are applied to the flutter of an isotropic panel in a supersonic airstream, in which case the nonlinearity is due to midplane stretching. The following brief survey serves as an introduction. For a comprehensive review, we refer the reader to Evan–Iwanowski (1976), Nayfeh and Mook (1979), Ibrahim (1985), Schmidt and Tondl (1986), and Nayfeh and Balachandran (1989, 1995).

Parametrically excited 2-DOF systems with quadratic nonlinearities and two-to-one autoparametric resonances were studied by Miles (1985), Nayfeh (1983b,c, 1987a), Nayfeh and Zavodney (1986), Streit et al. (1988), and Asrar (1991). Distributed-parameter systems with quadratic nonlinearities and two-to-one internal resonances were studied by Miles (1984), Ibrahim and Barr (1975), Holmes (1986), Nayfeh (1987b), Gu and Sethna (1987), and Nayfeh and Nayfeh (1990).

Tso and Asmis (1974) analyzed the response of a 2-DOF system with cubic nonlinearities for a principal parametric resonance of the first mode. Tezak et al. (1978) treated the nonlinear response of a hinged-clamped beam for principal and combination parametric resonances.

Parametrically excited systems with one-to-one internal resonances whose linear parts are

Received June 14, 1994; Accepted September 2, 1994.
Shock and Vibration, Vol. 2, No. 1, pp. 43–57 (1995)

CCC 1070-9622/95/020043-15

diagonal were studied by Asmis and Tso (1972), Ciliberto and Gollub (1985), Meron and Procaccia (1986), Simonelli and Gollub (1989), Feng and Sethna (1989), and Nayfeh and Pai (1989).

Parametrically excited systems having non-semisimple linear structures were studied by Fu and Nemat–Nasser (1972a,b), Nayfeh and Mook (1979), Tezak et al. (1982), Nayfeh (1983a), Namachchivaya and Malhotra (1992), and Nayfeh (1993). Fu and Nemat–Nasser used Floquet theory to analyze the response of linear multi-DOF systems with two repeated frequencies. Nayfeh and Mook (1979) used the method of multiple scales to analyze the response of linear multi-DOF systems with two repeated frequencies for principal, fundamental, and combination parametric resonances. Nayfeh (1983a) used the method of multiple scales to analyze the response of linear systems with three repeated frequencies. Tezak et al. (1982) used the method of multiple scales to determine the response of nonlinear multi-DOF systems with two repeated frequencies for principal parametric resonances. They applied the results to the flutter of a panel in a supersonic stream. Namachchivaya and Malhotra (1992) used the method of normal forms to analyze the response of general nonlinear 2-DOF systems with two repeated frequencies for a principal parametric resonance. They found some interesting phenomena, such as homoclinic bifurcations near the Bogdanov–Takens bifurcation point. Nayfeh (1993) used the methods of normal forms and multiple scales to derive normal forms for multi-DOF systems with two repeated frequencies and quadratic and cubic nonlinearities for principal, fundamental, and combination parametric resonances.

In this article we use the method of normal forms to reexamine the panel-flutter problem investigated by Tezak et al. (1982). We show that, in the case of a simply supported panel in a supersonic airstream, only heteroclinic orbits can be observed near the Bogdanov–Takens bifurcation point, whereas a homoclinic bifurcation can occur, resulting in a jump phenomenon. The theorem of Shilnikov (1970) is used to interpret these results. Some of the analytical results are verified by numerical integration of the governing equations.

EQUATION OF MOTION

The aeroelastic equations of motion for plates and shells are well established (Dowell, 1975; Dowell and Ilgamov, 1988). The motion of a panel under a harmonic in-plane load in a supersonic airstream is governed by the following equation (Dowell, 1975):

$$D\frac{\partial^4 w}{\partial x^4} - (N_x^E + N_x)\frac{\partial^2 w}{\partial x^2} + \rho_m h\frac{\partial^2 w}{\partial t^2} + \mu_m\frac{\partial w}{\partial t} = -\frac{\rho_\infty U_\infty^2}{M_\infty}\left(\frac{\partial w}{\partial x} + \frac{1}{U_\infty}\frac{\partial w}{\partial t}\right) \tag{1}$$

where

$$N_x = \frac{Eh}{2a}\int_0^a \left(\frac{\partial w}{\partial \xi}\right)^2 d\xi \tag{2}$$

is the tension due to the bending-induced stretching of the panel, D is the flexural rigidity, w is the transverse deflection, x is the stream-wise spatial coordinate, t is the time, N_x^E is the in-plane harmonic loading, E is the modulus of elasticity, h is the panel thickness, a is the panel length, and ρ_m and μ_m are the material density and damping, respectively. On the right-hand side of Eq. (1), piston theory is used to approximate the supersonic aerodynamic loads on the panel, where ρ_∞, U_∞, and M_∞ are the density, speed, and Mach number in the free stream.

Equation (1) can be rewritten in the following dimensionless form:

$$\frac{\partial^4 w^*}{\partial x^{*4}} + \frac{\partial^2 w^*}{\partial t^{*2}} + \lambda^*\frac{\partial w^*}{\partial x^*} = \left[R_x^* + \alpha^*\int_0^2 \left(\frac{\partial w^*}{\partial \xi^*}\right)^2 d\xi^*\right]\frac{\partial^2 w^*}{\partial x^{*2}} - 2\mu^*\frac{\partial w^*}{\partial t^*} \tag{3}$$

where

$$w^* = (a/h^2)w, \quad x^* = (2/a)x,$$
$$t^* = [4D^{1/2}/a^2(\rho_m h)^{1/2}]t, \quad \lambda^* = \rho_\infty U_\infty^2 a^3/8M_\infty D,$$
$$R_x^* = N_x^E a^2/4D = F\cos\Omega^* t^*,$$
$$\alpha^* = Eh^5/4a^2 D,$$
$$2\mu^* = (a^2/4(\rho_m h D)^{1/2})(\mu_m + \rho_\infty U_\infty/M_\infty).$$

Following the Galerkin procedure, Tezak et al. (1982) expressed the deflection as an expansion in terms of the linear free-vibration modes and obtained a system of ordinary differential equa-

tions for the time-dependent coefficients (also called modal amplitudes) in this expansion. For flutter, two natural frequencies coalesce and the corresponding modal amplitudes u_i are governed by equations having the following form:

$$\ddot{u}_1 + u_1 + 2\tilde{\mu}_1\dot{u}_1 + \tilde{\Lambda}_{11}u_1 + \tilde{\Lambda}_{12}u_2 + (2\cos\Omega\tau)(\tilde{f}_{11}u_1 + \tilde{f}_{12}u_2) + \tilde{\alpha}_{11}u_1^3 + \tilde{\alpha}_{12}u_1^2u_2 + \tilde{\alpha}_{13}u_1u_2^2 + \tilde{\alpha}_{14}u_2^3 = 0 \quad (4)$$

$$\ddot{u}_2 + u_1 + u_2 + 2\tilde{\mu}_2\dot{u}_2 + \tilde{\Lambda}_{21}u_1 + \tilde{\Lambda}_{22}u_2 + (2\cos\Omega\tau)(\tilde{f}_{21}u_1 + \tilde{f}_{22}u_2) + \tilde{\alpha}_{21}u_1^3 + \tilde{\alpha}_{22}u_1^2u_2 + \tilde{\alpha}_{23}u_1u_2^2 + \tilde{\alpha}_{24}u_2^3 = 0 \quad (5)$$

where $\tau = \omega^* t^*$ is the new independent variable; ω^* is the dimensionless natural frequency; the ratio of the excitation frequency to the natural frequency Ω is close to 2; the $\tilde{\Lambda}_{ij} = (\lambda^* - \lambda_c^*)C_{ij}$ are the aerodynamic detuning parameters; the C_{ij} are constants; λ_c^* is the critical value that causes two natural frequencies to merge and flutter to ensue; and the $\tilde{\mu}_i$, $\tilde{f}_{ij}$, and $\tilde{\alpha}_{ik}$ are constants related to the damping, in-plane loading, and nonlinear terms in Eq. (1), respectively. The case of a one-to-one internal resonance and a principal parametric excitation are studied.

Nayfeh and Mook (1979) showed that, in the presence of damping, all modes that are not directly or indirectly excited by an internal resonance decay with time.

METHOD OF SOLUTION

Tezak et al. (1982) used the method of multiple scales to obtain an approximate solution to Eqs. (4) and (5). One can obtain the same results by the method of normal forms, as we demonstrate in this section.

Scaling

Due to the nonsemisimple structure of the linear undamped operator, u_2 is much larger than u_1. Hence, after introducing ε as a bookkeeping device, one assumes that

$$u_1 = \varepsilon v_1, \quad u_2 = \varepsilon^{1-\delta_1}v_2, \quad \tilde{\mu}_i = \varepsilon^{\delta_2}\mu_i$$
$$\tilde{\Lambda}_{ij} = \varepsilon^{\delta_3}\Lambda_{ij}, \quad \tilde{f}_{ij} = \varepsilon^{\delta_4}f_{ij}, \quad \tilde{\alpha}_{ik} = \varepsilon^{\delta_5}\alpha_{ik} \quad (6)$$

for $i = 1, 2, j = 1, 2, k = 1, 2, 3, 4$, where the δ_m are unspecified (for the present) positive constants. Substituting Eq. (6) into Eqs. (4) and (5) yields

$$\ddot{v}_1 + v_1 + \varepsilon^{\delta_2}2\mu_1\dot{v}_1 + \varepsilon^{\delta_3}(\Lambda_{11}v_1 + \varepsilon^{-\delta_1}\Lambda_{12}v_2) + (2\cos\Omega\tau)\varepsilon^{\delta_4}(f_{11}v_1 + \varepsilon^{-\delta_1}f_{12}v_2) + \varepsilon^{\delta_5+2}(\alpha_{11}v_1^3 + \varepsilon^{-\delta_1}\alpha_{12}v_1^2v_2 + \varepsilon^{-2\delta_1}\alpha_{13}v_1v_2^2 + \varepsilon^{-3\delta_1}\alpha_{14}v_2^3) = 0 \quad (7)$$

$$\ddot{v}_2 + \varepsilon^{\delta_1}v_1 + v_2 + \varepsilon^{\delta_2}2\mu_2\dot{v}_2 + \varepsilon^{\delta_3}(\varepsilon^{\delta_1}\Lambda_{21}v_1 + \Lambda_{22}v_2) + (2\cos\Omega\tau)\varepsilon^{\delta_4}(\varepsilon^{\delta_1}f_{21}v_1 + f_{22}v_2) + \varepsilon^{\delta_5+2}(\varepsilon^{\delta_1}\alpha_{21}v_1^3 + \alpha_{22}v_1^2v_2 + \varepsilon^{-\delta_1}\alpha_{23}v_1v_2^2 + \varepsilon^{-2\delta_1}\alpha_{24}v_2^3) = 0. \quad (8)$$

Keeping only the dominant terms, we have

$$\ddot{v}_1 + v_1 + \varepsilon^{\delta_2}2\mu_1\dot{v}_1 + \varepsilon^{\delta_3-\delta_1}\Lambda_{12}v_2 + \varepsilon^{\delta_4-\delta_1}(2\cos\Omega\tau)f_{12}v_2 + \varepsilon^{\delta_5+2-3\delta_1}\alpha_{14}v_2^3 + \cdots = 0 \quad (9)$$

$$\ddot{v}_2 + \varepsilon^{\delta_1}v_1 + v_2 + \varepsilon^{\delta_2}2\mu_2\dot{v}_2 + \cdots = 0. \quad (10)$$

To make the damping, aerodynamic loading, parametric resonance, and nonlinearity interact in the first approximation, we let

$$\delta_2 = \delta_3 - \delta_1 = \delta_4 - \delta_1 = \delta_5 + 2 - 3\delta_1 = \delta_1. \quad (11)$$

Hence, for an arbitrary δ_1, say 1,

$$\delta_2 = 1, \quad \delta_3 = 2, \quad \delta_4 = 2, \quad \text{and} \quad \delta_5 = 2 \quad (12)$$

and the scaled Eqs. (9) and (10) become

$$\ddot{v}_1 + v_1 + 2\varepsilon\mu_1\dot{v}_1 + \varepsilon\Lambda_{12}v_2 + \varepsilon(2\cos\Omega\tau)f_{12}v_2 + \varepsilon\alpha_{14}v_2^3 + \cdots = 0 \quad (13)$$

$$\ddot{v}_2 + \varepsilon v_1 + v_2 + 2\varepsilon\mu_2\dot{v}_2 + \cdots = 0. \quad (14)$$

Method of Normal Forms

To simplify Eqs. (13) and (14), using the method of normal forms (Nayfeh, 1993), we first recast them in complex-valued form using the following transformation:

$$v_j = \eta_j + \bar{\eta}_j, \quad \dot{v}_j = i(\eta_j - \bar{\eta}_j), \quad j = 1, 2 \quad (15)$$

where $\bar{\eta}_j$ is the complex conjugate of η_j. Solving for η_j and $\bar{\eta}_j$, we obtain

$$\eta_j = \frac{1}{2}(v_j - i\dot{v}_j) \quad \text{and} \quad \bar{\eta}_j = \frac{1}{2}(v_j + i\dot{v}_j). \quad (16)$$

Differentiating the first of Eqs. (16) with respect to τ and using Eqs. (13)–(15), we find

$$\dot{\eta}_1 = i\eta_1 + \frac{1}{2}\varepsilon i[i2\mu_1(\eta_1 - \bar{\eta}_1) + \Lambda_{12}(\eta_2 + \bar{\eta}_2) + f_{12}(z + \bar{z})(\eta_2 + \bar{\eta}_2) + \alpha_{14}(\eta_2 + \bar{\eta}_2)^3] + \cdots \tag{17}$$

$$\dot{\eta}_2 = i\eta_2 + \frac{1}{2}\varepsilon i[\eta_1 + \bar{\eta}_1 + i2\mu_2(\eta_2 - \bar{\eta}_2)] + \cdots \tag{18}$$

where $z = e^{i\Omega\tau}$. Next, we introduce the near-identity transformation

$$\eta_j = \xi_j + \varepsilon h_j(\xi_m, \bar{\xi}_m, z, \bar{z}) + \cdots, \quad m = 1, 2 \quad \text{for each} \quad j = 1, 2 \tag{19}$$

into Eqs. (17) and (18) and choose the h_j so that the resulting equations take the simplest possible form, the so-called normal form:

$$\dot{\xi}_j = i\xi_j + \varepsilon g_j(\xi_m, \bar{\xi}_m, z, \bar{z}) + \cdots, \quad m = 1, 2 \quad \text{for each} \quad j = 1, 2 \tag{20}$$

where the g_j consist of the resonance and near-resonance terms. After substituting Eqs. (19) and (20) into Eq. (17) and equating the coefficients of ε, we obtain

$$g_1 + i\left(\frac{\partial h_1}{\partial \xi_1}\xi_1 - \frac{\partial h_1}{\partial \bar{\xi}_1}\bar{\xi}_1 + \frac{\partial h_1}{\partial \xi_2}\xi_2 - \frac{\partial h_1}{\partial \bar{\xi}_2}\bar{\xi}_2\right) + i\Omega\left(\frac{\partial h_1}{\partial z}z - \frac{\partial h_1}{\partial \bar{z}}\bar{z}\right) = ih_1 - \mu_1(\xi_1 - \bar{\xi}_1) + \frac{1}{2}i[\Lambda_{12}(\xi_2 + \bar{\xi}_2) + f_{12}(z + \bar{z})(\xi_2 + \bar{\xi}_2) + \alpha_{14}(\xi_2 + \bar{\xi}_2)^3]. \tag{21}$$

Choosing h_1 to eliminate the nonresonance terms in Eq. (21) leaves g_1 with the resonance and near-resonance terms; that is,

$$g_1 = -\mu_1\xi_1 + \frac{1}{2}i(\Lambda_{12}\xi_2 + 3\alpha_{14}\xi_2^2\bar{\xi}_2 + f_{12}z\bar{\xi}_2). \tag{22}$$

The term proportional to $z\bar{\xi}_2$ is a near-resonance term because $\Omega \approx 2$ and the rest of the terms on the right-hand side of Eq. (22) are resonance terms. After substituting Eqs. (19) and (20) into Eq. (18), equating the coefficients of ε, and choosing h_2 to eliminate the nonresonance terms, we obtain

$$g_2 = -\mu_2\xi_2 + \frac{1}{2}i\xi_1. \tag{23}$$

Substituting Eqs. (22) and (23) into Eq. (20) yields the normal form

$$\dot{\xi}_1 = i\xi_1 - \varepsilon\mu_1\xi_1 + \frac{1}{2}i\varepsilon(\Lambda_{12}\xi_2 + 3\alpha_{14}\xi_2^2\bar{\xi}_2 + f_{12}z\bar{\xi}_2) \tag{24}$$

$$\dot{\xi}_2 = i\xi_2 - \varepsilon\mu_2\xi_2 + \frac{1}{2}i\varepsilon\xi_1. \tag{25}$$

Next, we introduce a detuning parameter σ defined by

$$\Omega = 2 + \varepsilon\sigma \tag{26}$$

where $\varepsilon\sigma$ is small compared with 1. Moreover, we express the ξ_j in the polar form

$$\xi_j = \frac{1}{2}a_j e^{i(\tau+\beta_j)} \tag{27}$$

recall that $z = e^{i\Omega\tau}$, separate Eqs. (24) and (25) into real and imaginary parts, and obtain

$$a_1' = -\mu_1 a_1 - \left(\frac{1}{2}\Lambda_{12}a_2 + \frac{3}{8}\alpha_{14}a_2^3\right)\sin\gamma_1 - \frac{1}{2}f_{12}a_2\sin\gamma_2 \tag{28}$$

$$a_1\beta_1' = \left(\frac{1}{2}\Lambda_{12}a_2 + \frac{3}{8}\alpha_{14}a_2^3\right)\cos\gamma_1 + \frac{1}{2}f_{12}a_2\cos\gamma_2 \tag{29}$$

$$a_2' = -\mu_2 a_2 + \frac{1}{2}a_1\sin\gamma_1 \tag{30}$$

$$a_2\beta_2' = \frac{1}{2}a_1\cos\gamma_1 \tag{31}$$

where the prime is the derivative with respect to $T_1 = \varepsilon\tau$,

$$\gamma_1 = \beta_2 - \beta_1 \quad \text{and} \quad \gamma_2 = \sigma T_1 - \beta_2 - \beta_1. \tag{32}$$

A comparison between the numerical time integration of the modulation equations and the original governing equations is shown in Figs. 1–3. In Fig. 1, we show the effect of ε, which appears in the scaling process. Clearly, the accuracy of the perturbation solution improves as ε decreases. Good agreement between the perturbation and exact solution is reached when $\varepsilon = 0.01$, which is also used for the results obtained in Figs. 2 and 3.

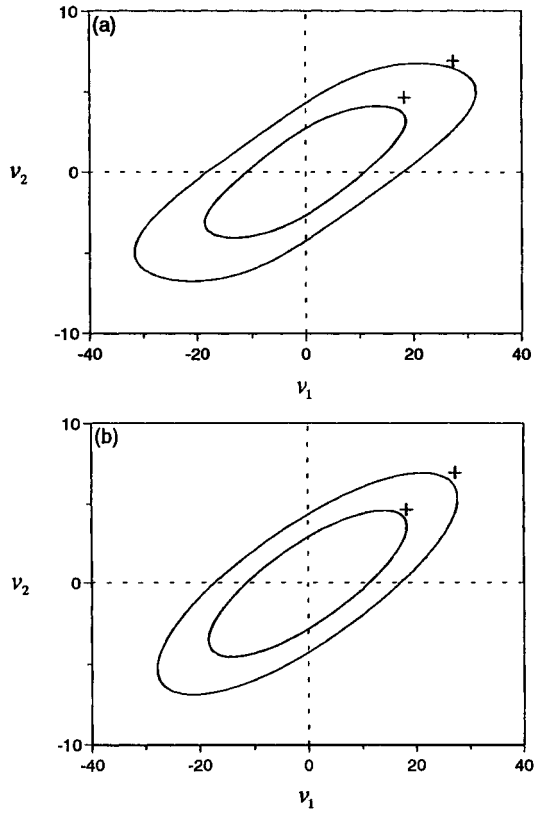

FIGURE 1 Comparison between the numerical time integration of the modulation equations (+) and the original governing equations for $(\Lambda, F) = (0, 500)$ and $(0, 1000)$ (outer loop); (a) $\varepsilon = 0.1$; (b) $\varepsilon = 0.01$.

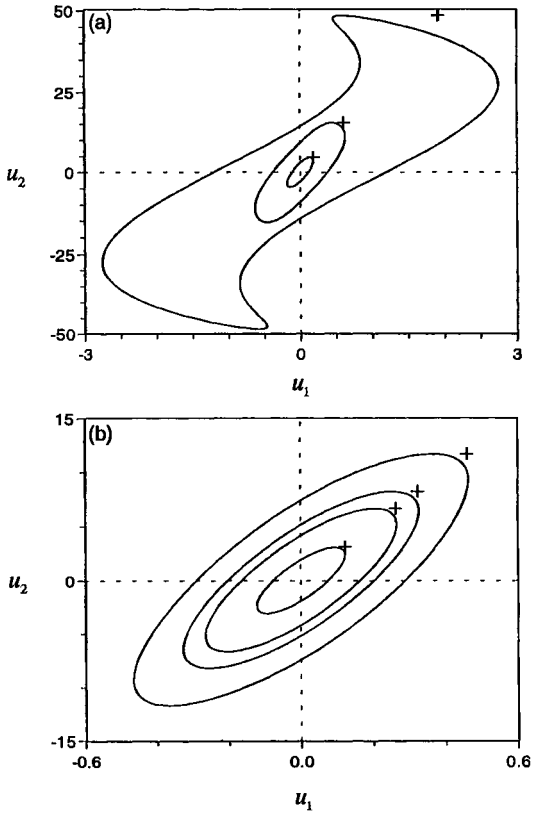

FIGURE 2 Comparison between the numerical time integration of the modulation equations (+) and the original governing equations for $\varepsilon = 0.01$; (a) $\Lambda = 0$, $F = 500$, 5000, and 50000 (outer loop); (b) $F = 500$, $\Lambda = -500$, 1000, 2000, and 5000 (outer loop).

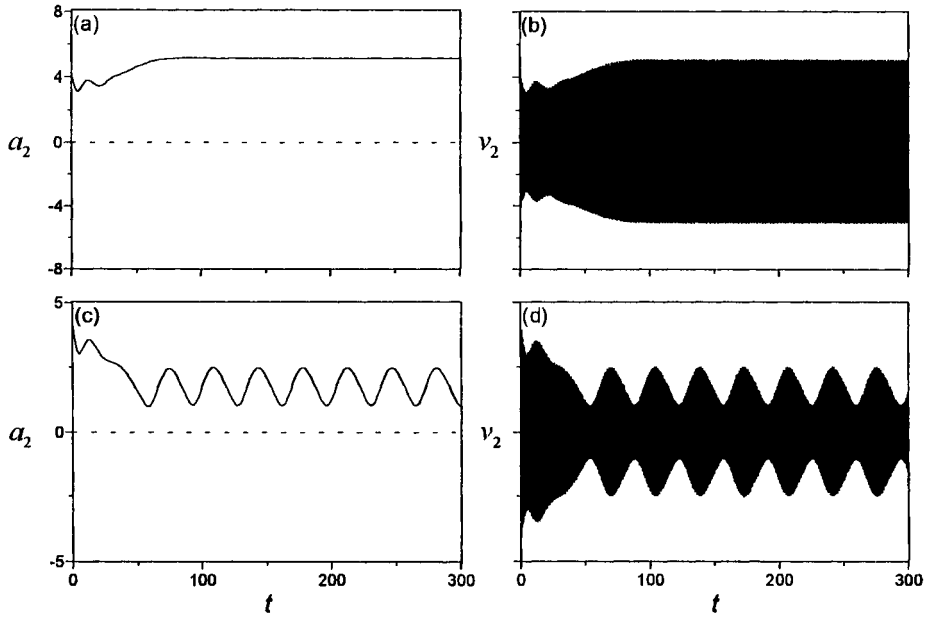

FIGURE 3 Comparison between the numerical time integration of the modulation equations (left) and the original governing equations (right). $(\Lambda, F) = (600, 379)$ for (a) and (b); $(\Lambda, F) = (600, 329)$ for (c) and (d).

By introducing this ε, one can observe that u_2 is much larger than u_1, which is consistent with the inherent nonsemisimple structure of the system under investigation.

EQUILIBRIUM SOLUTIONS AND THEIR STABILITY

The equilibrium solutions of Eqs. (28)–(32) correspond to $a_j' = 0$ and $\gamma_j' = 0$. There are two possibilities: a trivial solution:

$$a_1 = a_2 = 0 \tag{33}$$

and a nontrivial solution:

$$a_1 = a_2 \sqrt{\sigma^2 + 4\mu_2^2} \tag{34}$$

$$a_2^2 = \frac{4}{3\alpha_{14}} \{-\Lambda_{12} + \sigma^2 - 4\mu_1\mu_2 \pm \sqrt{f_{12}^2 - 4\sigma^2(\mu_1 + \mu_2)^2}\}. \tag{35}$$

In the example considered below, α_{14} is positive and Λ_{12} decreases with M_∞ and is zero at the critical M_∞.

The trivial solution always exists, although it may not always be stable. The nontrivial solution exists when a_2^2 is positive. One requirement is

$$f_{12} \geq 2|\sigma(\mu_1 + \mu_2)|. \tag{36}$$

In addition, when

$$\sigma^2 - \Lambda_{12} - 4\mu_1\mu_2 > \sqrt{f_{12}^2 - 4\sigma^2(\mu_1 + \mu_2)^2} \tag{37a}$$

there are two possible nonzero values for a_2^2 and when

$$\sqrt{f_{12}^2 - 4\sigma^2(\mu_1 + \mu_2)^2} > |\sigma^2 - \Lambda_{12} - 4\mu_1\mu_2| \tag{37b}$$

there is only one nonzero value for a_2^2. Condition (37b) applies for both positive and negative values of $\sigma^2 - \Lambda_{12} - 4\mu_1\mu_2$.

Next, we examine the stability of the various solutions. We are particularly interested in the boundaries separating the stable combinations of parameters from the unstable ones.

Stability of Trivial Solution

Determining the limits of stability for the trivial solution is equivalent to determining the flutter boundaries. We introduce the Cartesian form

$$\xi_j = \frac{1}{2}(p_j - iq_j)e^{i(1+(1/2)\varepsilon\sigma)\tau}, \quad j = 1, 2 \tag{38}$$

to transform the nonautonomous system (24) and (25) into the four-dimensional autonomous system

$$\underline{x}' = L\underline{x} + \underline{N}(\underline{x}) \tag{39}$$

where

$$\underline{x} = \begin{bmatrix} p_1 \\ q_1 \\ p_2 \\ q_2 \end{bmatrix}, \quad \underline{N} = \frac{3}{8}\alpha_{14}(p_2^2 + q_2^2)\begin{bmatrix} q_2 \\ -p_2 \\ 0 \\ 0 \end{bmatrix}, \tag{40}$$

and

$$L = \frac{1}{2}\begin{bmatrix} -2\mu_1 & -\sigma & 0 & \Lambda_{12} - f_{12} \\ \sigma & -2\mu_1 & -\Lambda_{12} - f_{12} & 0 \\ 0 & 1 & -2\mu_2 & -\sigma \\ -1 & 0 & \sigma & -2\mu_2 \end{bmatrix}. \tag{41}$$

The eigenvalues λ of the matrix L satisfy the characteristic equation

$$\lambda^4 + r_1\lambda^3 + r_2\lambda^2 + r_3\lambda + r_4 = 0 \tag{42}$$

where

$$r_1 = 2(\mu_1 + \mu_2) \tag{43a}$$

$$r_2 = \mu_1^2 + \mu_2^2 + 4\mu_1\mu_2 + \frac{1}{2}(\Lambda_{12} + \sigma^2) \tag{43b}$$

$$r_3 = (\mu_1 + \mu_2)\left(2\mu_1\mu_2 + \frac{1}{2}\Lambda_{12} + \frac{1}{2}\sigma^2\right) \tag{43c}$$

$$r_4 = \frac{1}{4}\sigma^2(\mu_1 + \mu_2)^2 + \left(\mu_1\mu_2 + \frac{1}{4}\Lambda_{12} - \frac{1}{4}\sigma^2\right)^2 - \frac{1}{16}f_{12}^2. \tag{43d}$$

According to the Routh–Hurwitz criterion, at least one root of Eq. (42) has a positive real part if at least one of the following conditions is not satisfied:

$$r_1 > 0, \quad r_1 r_2 - r_3 > 0,$$
$$r_3(r_1 r_2 - r_3) - r_1^2 r_4 > 0, \quad r_4 > 0. \tag{44}$$

The flutter boundaries separating stable and unstable regions for the case of a simply supported panel can then be constructed to form the bifurcation diagram, as shown in Fig. 4. Stable trivial solutions exist in regions I and II only. As a control parameter is varied, the trivial equilibrium solution can undergo a variety of bifurcations. The qualitative dynamical behavior near these bifurcation curves can be analyzed by a combination of center manifold theory and the method of normal forms.

Static Bifurcations of Trivial Solution. The P curve in Fig. 4 corresponds to the condition $r_4 = 0$, where r_4 is defined in Eq. (43d). Thus, along this bifurcation curve, the linear operator L has a zero eigenvalue. As F crosses the P curve directly from region I into region III at a fixed Λ, a supercritical pitchfork bifurcation occurs, which can be identified by the normal form (Nayfeh and Balachandran, 1994)

$$y' = \varepsilon_1(F - F_{cr})y + \alpha_1 y^3, \qquad \varepsilon_1 > 0 \quad \text{and} \quad \alpha_1 < 0 \tag{45}$$

where F_{cr} is the bifurcation value. If F crosses from region II into region III, a subcritical pitchfork bifurcation occurs. It can be identified by the normal form (Nayfeh and Balachandran, 1994)

$$y' = \varepsilon_2(F - F_{cr})y + \alpha_2 y^3, \qquad \varepsilon_2 > 0 \quad \text{and} \quad \alpha_2 > 0. \tag{46}$$

In the case of supercritical bifurcation, the stable trivial solution loses stability and gives way to a stable nontrivial constant solution (or periodic solution of the original system) that smoothly grows with F, as shown in Fig. 5(a), where $(\varepsilon_1, \alpha_1) = (0.0033, -0.001)$ when $(\Lambda, F_{cr}) = (-300, 332.92)$. In the case of subcritical bifurcation, the solution jumps from a trivial to a nontrivial value as F increases past the bifurcation value, as shown in Fig. 5(b), where $(\varepsilon_2, \alpha_2) = (0.0058, 0.0028)$ when $(\Lambda, F_{cr}) = (100, 346.79)$.

Hopf Bifurcation of Trivial Solution. The H curve in Fig. 4 corresponds to the condition $r_3(r_1 r_2 - r_3) - r_1^2 r_4 = 0$, where the r_j are defined in Eqs. (43). The linear operator L has a pair of purely imaginary eigenvalues along this bifurcation curve. As Λ crosses the H curve from region I into region IV or from region II into region V at a fixed F, a supercritical Hopf bifurcation occurs that can be identified by the normal form (Nayfeh and Balachandran, 1994)

$$r' = \varepsilon_3(\Lambda - \Lambda_{cr})r + \alpha_3 r^3, \qquad \varepsilon_3 > 0 \quad \text{and} \quad \alpha_3 < 0 \tag{47a}$$

$$\theta' = \rho + \alpha_4 r^2, \quad \rho^2 = r_3/r_1 \quad \text{and} \quad \alpha_4 < 0 \tag{47b}$$

where Λ_{cr} is the bifurcation value. In Fig. 6(a,b), the variation of the amplitude of the second mode with the aerodynamic detuning for two values of the excitation amplitude is shown.

When $F = 200$ and Λ is increased slowly, the stable trivial solution loses stability across the Hopf bifurcation curve at $\Lambda_{cr} \approx 326.41$, where $(\varepsilon_3, \alpha_3) = (0.0026, -0.0475)$ and $(\rho, \alpha_4) = (1.423, -0.0053)$. The amplitude of the periodic solution of the modulation equations (or quasiperiodic solution of the original system) gradually grows with increasing Λ, as shown in Figs. 6(a) and 7(c,d).

We show the results for $F = 350$ in Fig. 6(b). When Λ is increased from a low value, the trivial solution loses stability at $\Lambda \approx -416$ (point B) and a stable nontrivial constant solution (which passes through points F and A) starts to grow as Λ continues to increase. When $\Lambda \approx 118$ (point E), a second, unstable nontrivial constant solution is

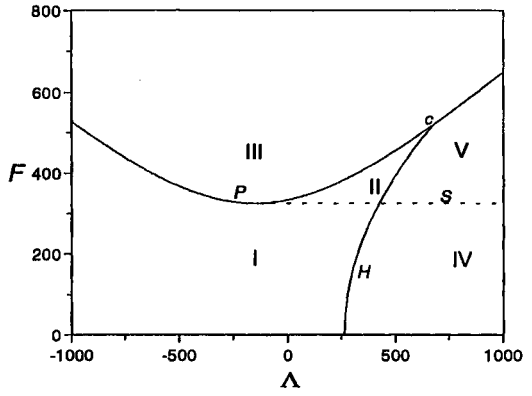

FIGURE 4 Various regions of interest obtained from the linear and nonlinear stability analyses for a simply supported panel, $\omega^* = 8.1076$, $\sigma = 25/\omega^*$, $\mu_1 = \mu_2 = 10/\omega^*$, $\Lambda_{12} = -99.2\Lambda/\omega^{*4}$, $f_{12} = 202.5F/\omega^{*4}$, and $\alpha_{14} = 5729/\omega^{*4}$. The P and H curves define the linear flutter boundaries. The P curve corresponds to pitchfork bifurcations, the H curve corresponds to Hopf bifurcations, and the S curve corresponds to saddle-node bifurcations.

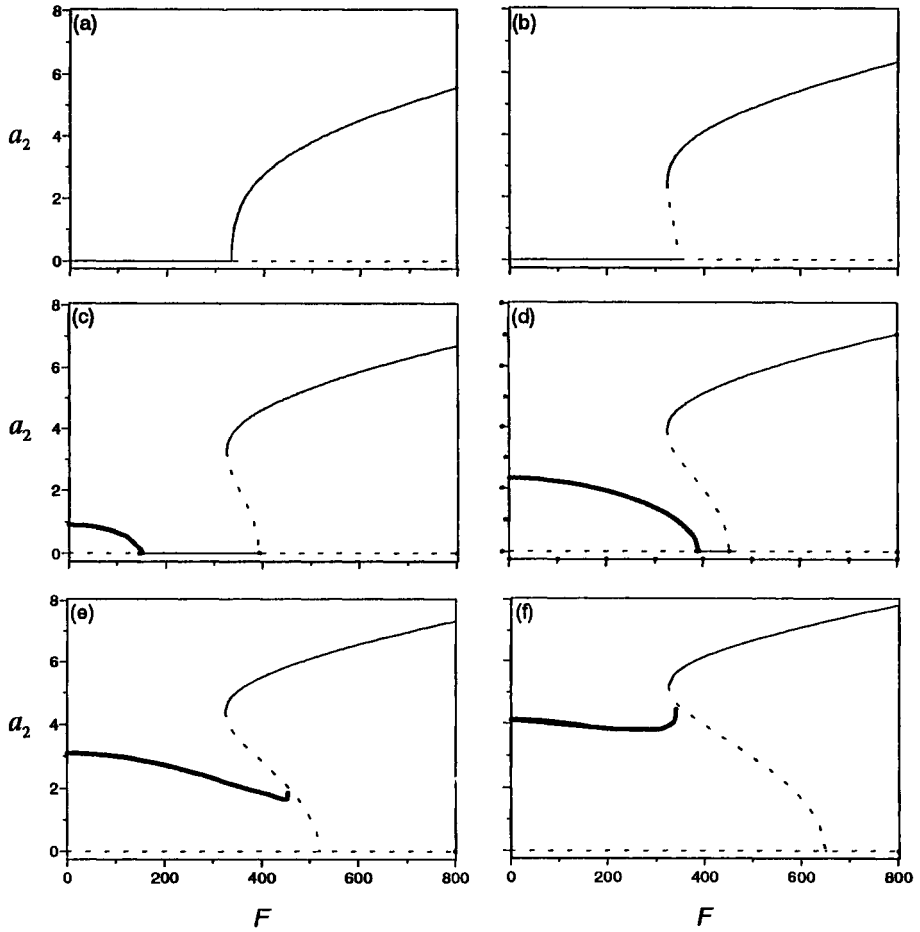

FIGURE 5 Variation of the amplitude of the second mode a_2 with the amplitude of the parametric excitation: (a) $\Lambda = -300$; (b) $\Lambda = 100$; (c) $\Lambda = 300$; (d) $\Lambda = 500$; (e) $\Lambda = 679.2$; and (f) $\Lambda = 1000$. Thin-solid lines denote stable constant solutions, dotted lines denote unstable constant solutions, and thick-solid lines denote mean amplitude of the periodic solutions.

possible and the unstable trivial solution regains its stability. It remains stable until $\Lambda \approx 453$ (point D), where $(\varepsilon_3, \alpha_3) = (0.0032, -0.04)$ and $(\rho, \alpha_4) = (1.140, -0.0158)$ a supercritical Hopf bifurcation occurs and a periodic solution of the modulation equations emerges. The amplitude of the periodic (limit-cycle) solution of the modulation equations grows as Λ continues to increase, as indicated by the heavy line from D to C in Fig. 6(b). In the region of multiple stable solutions, the response depends on the initial conditions.

Starting from a stable nontrivial constant solution at a large value of Λ, point A in Fig. 6(b), and then gradually decreasing Λ, one finds that the amplitude of the nontrivial solution decreases through point F until a stable trivial solution is reached at point B. Starting from a periodic solution at a large value of Λ, point C, and gradually decreasing Λ, one finds that the amplitude of the limit-cycle solution decreases until a reverse Hopf bifurcation to a stable trivial solution occurs at point D. However, as Λ continues to decrease, a jump occurs at the reverse pitchfork bifurcation, point E, to the stable nontrivial solution, point F, which is the only realizable solution. As Λ decreases further, the solution follows the stable branch from point F to point B.

Stability of Nontrivial Solutions

The Jacobian matrix of the autonomous system defined by Eqs. (28)–(32) evaluated at the nontri-

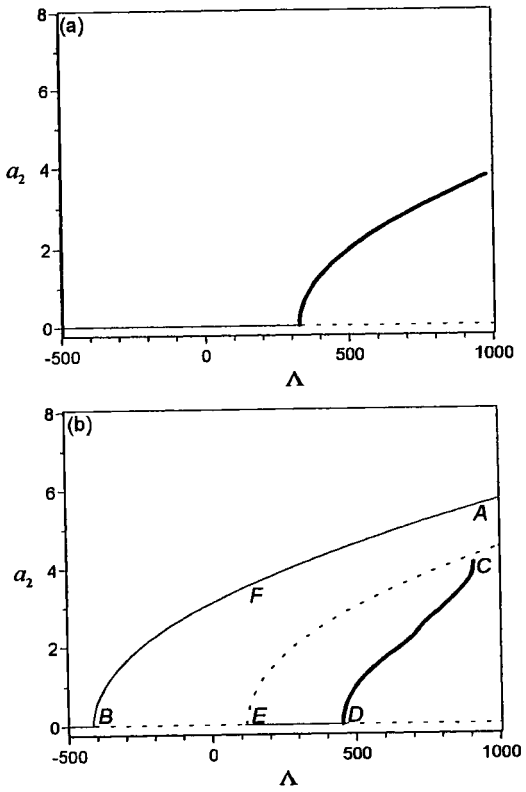

FIGURE 6 Variation of the amplitude of the second mode a_2 with the aerodynamic detuning: (a) $F = 200$; (b) $F = 350$. Thin-solid lines denote stable constant solutions, dotted lines denote unstable constant solutions, and thick-solid lines denote the mean amplitude of the periodic solutions.

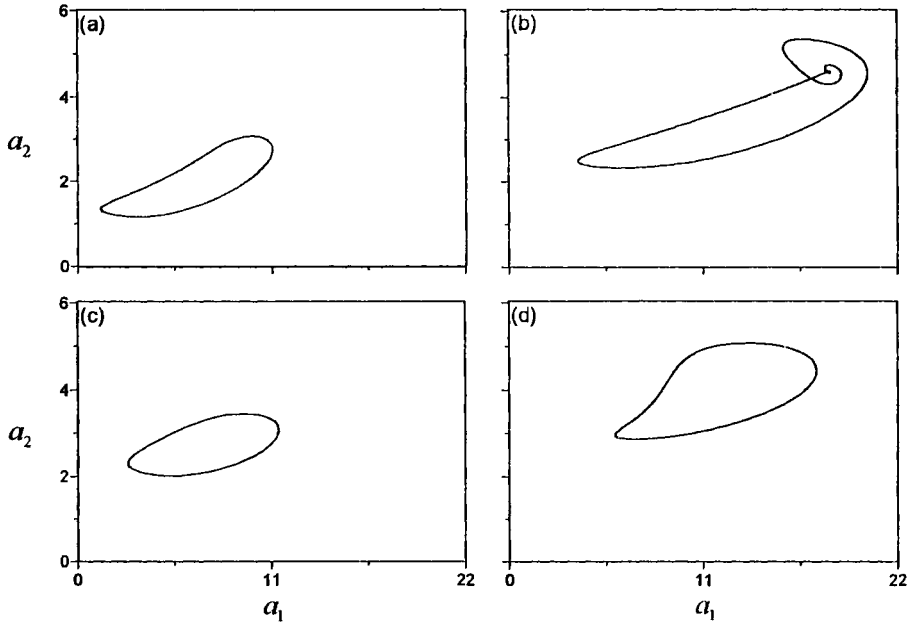

FIGURE 7 A two-dimensional projection of the phase portrait onto the $a_2 - a_1$ plane: (Λ, F) = (a) (679.2, 340); (b) (1000, 340); (c) (679.2, 200); and (d) (1000, 200).

vial fixed points can be expressed as

$$J = \begin{bmatrix} -\mu_1 & J_{12} & J_{13} & -\frac{1}{2} f_{12} a_2 \cos\gamma_2 \\ \frac{1}{2}\sin\gamma_1 & -\mu_2 & \frac{1}{2} a_1 \cos\gamma_1 & 0 \\ \frac{1}{a_2}\cos\gamma_1 & J_{32} & J_{33} & \frac{f_{12}}{2a_1} a_2 \sin\gamma_2 \\ \frac{\sigma}{a_1} - \frac{1}{a_2}\cos\gamma_1 & \frac{\sigma}{a_2} + J_{32} & \frac{a_1}{a_2}\sin\gamma_1 + J_{33} & \frac{f_{12}}{2a_1} a_2 \sin\gamma_2 \end{bmatrix} \tag{48a}$$

where

$$J_{12} = -\frac{1}{2}\left(\Lambda_{12} + \frac{9}{4}\alpha_{14} a_2^2\right)\sin\gamma_1 - \frac{1}{2} f_{12}\sin\gamma_2 \tag{48b}$$

$$J_{13} = -\frac{1}{2}\left(\Lambda_{12} + \frac{3}{4}\alpha_{14} a_2^2\right) a_2 \cos\gamma_1 \tag{48c}$$

$$J_{32} = -\frac{1}{a_1}\left[\left(\Lambda_{12} + \frac{3}{2}\alpha_{14} a_2^2\right)\cos\gamma_1 + f_{12}\cos\gamma_2\right] \tag{48d}$$

$$J_{33} = \left(-\frac{a_1}{2a_2} + \frac{\Lambda_{12}}{2a_1} a_2 + \frac{3\alpha_{14}}{8a_1} a_2^3\right)\sin\gamma_1. \tag{48e}$$

The stability of a nontrivial equilibrium solution depends on the real parts of the eigenvalues of the matrix J. If the real part of each eigenvalue is negative, the corresponding equilibrium solution is asymptotically stable. If the real part of at least one of the eigenvalues is positive, the corresponding equilibrium solution is unstable. In regions II and V of Fig. 4, there are two nontrivial constant solutions: one is stable and one is unstable. And in region III, there is one nontrivial constant solution, which is stable. If the equilibrium solution becomes nonhyperbolic, a similar bifurcation analysis can be conducted near the nontrivial fixed point by using the center manifold theory and the method of normal forms. As F is decreased across the line S, where $F = F_{cr}$, between regions I and II (or IV and V) for a fixed Λ, one real eigenvalue becomes positive and a saddle-node bifurcation occurs; it can be identified by the normal form

$$y' = \varepsilon_4(F - F_{cr}) - y^2, \quad \varepsilon_4 > 0. \tag{49}$$

In Fig. 5(b–f), as F decreases past the bifurcation point, the stable nontrivial constant solution no longer exists and either jumps down to a stable trivial constant solution or a_2 becomes a periodic function. The unstable branch of nontrivial constant solutions is unrealizable in both numerical and physical experiments.

Stability of Periodic Solutions

Using Floquet theory to check the stability of the periodic solutions in regions IV and V, one finds that only stable periodic solutions exist in region IV, whereas stable periodic solutions and stable nontrivial constant solutions coexist in part of region V, as shown in Figs. 5(e,f) and 6. In the latter case, the response depends on the initial conditions. In Figs. 5(c,d) and 8, the mean value of the amplitude of the periodic solution decreases while its period increases as F increases, and eventually a reverse Hopf bifurcation produces a stable trivial solution. In Fig. 5(e,f), when Λ is either near the value where the Bogdanov–Takens bifurcation occurs or away from the Hopf-bifurcation curve, the mean value of the amplitude of the periodic solution first decreases with F, then starts to increase somewhere beneath the unstable branch of nontrivial constant solutions (saddles). At this point, the periodic solution is stable in a sense that the corresponding Floquet multipliers lie within the unit circle. However, as shown in Fig. 8 for fixed values of Λ, the period of the limit cycle tends to infinity as F increases, suggesting the occurrence of a homoclinic orbit.

If a system has an orbit homoclinic to a saddle focus, which has one positive real eigenvalue λ_1, $\lambda_2 = \bar{\lambda}_3 = -\alpha + i\omega$, and Real$(-\lambda_i) > \alpha$ for $i = 4, 5, \ldots, n$, where α and ω are positive, Shilnikov (1970) showed that the system has a stable periodic orbit on one side of the homoclinic orbit and

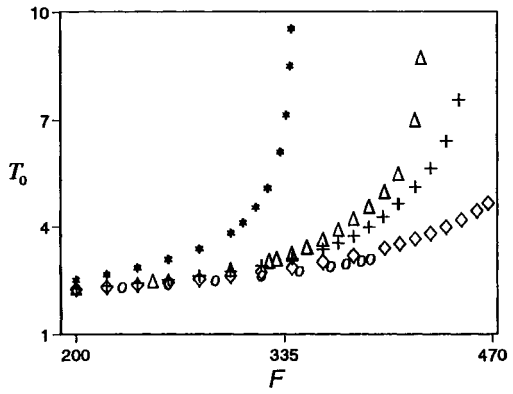

FIGURE 8 Variation of the period of the periodic motion with the amplitude of the parametric excitation. (O) $\Lambda = 500$; ($\diamond$) $\Lambda = 600$; (+) $\Lambda = 679$; (Δ) $\Lambda = 700$; (*) $\Lambda = 1000$.

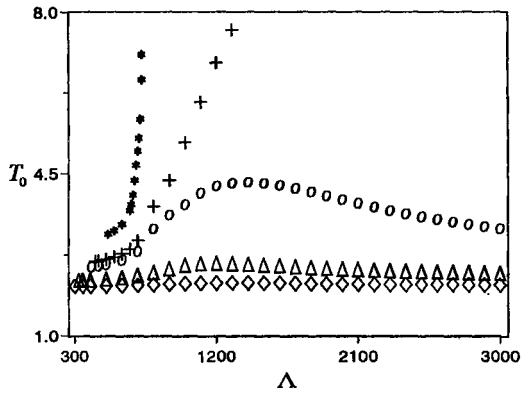

FIGURE 10 Variation of the period of the periodic motion with the aerodynamic detuning. ($\diamond$) $F = 100$; (Δ) $F = 200$; (O) $F = 300$; (+) $F = 325$; (*) $F = 400$.

no recurrent behavior on the other if the eigenvalues of this saddle satisfy the inequality

$$\delta \equiv \alpha/\lambda_1 > 1, \tag{50}$$

which is the case in the current study.

The projections of the unstable manifolds of the saddle focus are shown in Fig. 9 for $\Lambda = 1000$. Before the homoclinicity condition is reached, the unstable manifold leads to a limit cycle in one direction and to a sink in the other, as shown in part (a) for $F = 330$. As F increases, the limit cycle grows and its period increases, as shown in part (b) for $F = 335$. At $F = F_h \approx 340.853$, the periodic orbit passes through the saddle focus, forming the homoclinic orbit. The eigenvalues of the saddle focus are $\lambda_1 = 0.4656$, $\lambda_{2,3} = -1.2334 \pm 4.2036i$, and $\lambda_4 = -2.9324$. Hence, $\delta = 2.649 > 1$. Therefore, according to the Shilnikov theorem, when $F < F_h$, the system has a stable limit cycle, and when $F > F_h$ it has no recurrent behavior, explaining the results in Fig. 9.

In Fig. 10, when Λ increases from approxi-

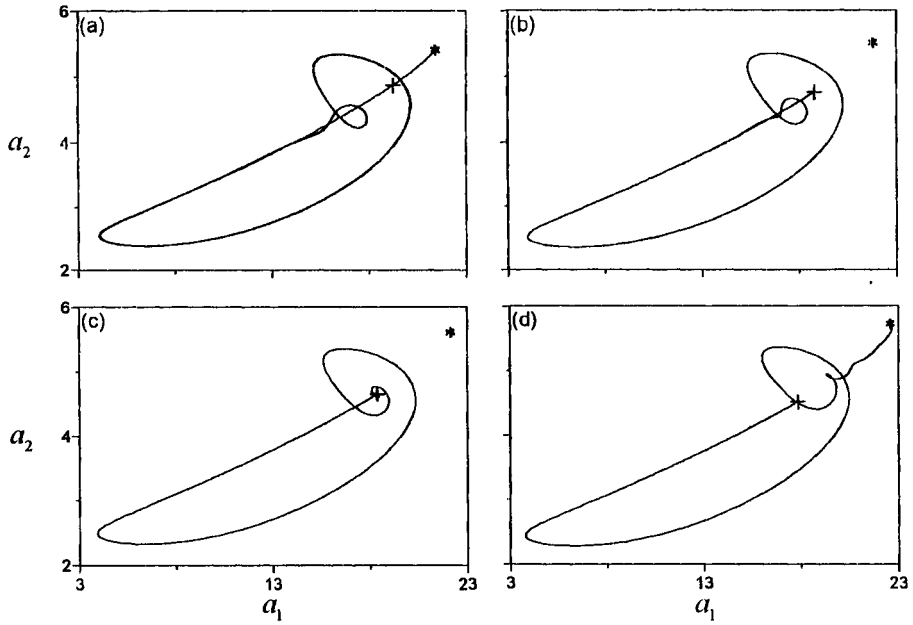

FIGURE 9 A two-dimensional projection of an unstable manifold onto the $a_2 - a_1$ plane for $\Lambda = 1000$ and $F =$ (a) 330 (both directions are included); (b) 335; (c) 340.853; (d) 350. (+) denotes a saddle and (*) denotes a sink.

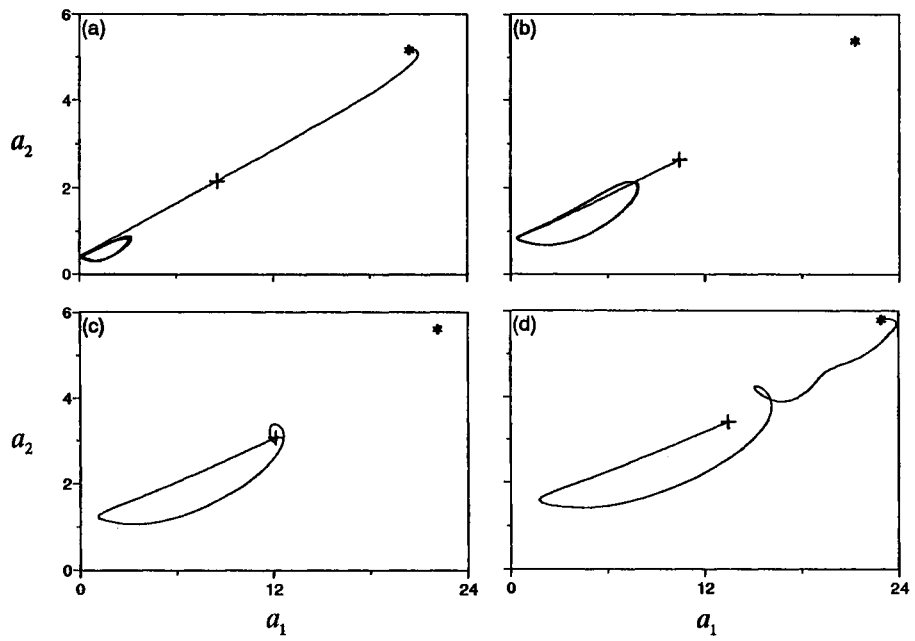

FIGURE 11 A two-dimensional projection of an unstable manifold onto the $a_2 - a_1$ plane for $F = 400$ and Λ = (a) 530 (both directions are included); (b) 630; (c) 734.161; (d) 830. (+) denotes a saddle and (*) denotes a sink.

mately 510.5 for $F = 400$, where a supercritical Hopf bifurcation occurs and a limit cycle is born, the period of the limit cycle increases and tends to infinity as $\Lambda \to \Lambda_h \approx 734.16$. In Fig. 11(a) for $\Lambda = 530$, the unstable manifold of the saddle leads to a limit cycle in one direction and to a sink in the other. As Λ increases further, the limit cycle grows and approaches the homoclinic orbit, as shown in part (b) for $\Lambda = 630$ and part (c) for $\Lambda = 734.1614$, respectively. The eigenvalues of the saddle focus at $\Lambda = \Lambda_h$, where a homoclinic orbit occurs, are $\lambda_1 = 0.7262$, $\lambda_{2,3} = -1.2334 \pm 3.0807i$, and $\lambda_4 = -3.193$. Clearly, $\delta = 1.698 > 1$. Therefore, according to the Shilnikov theorem, the system has a stable limit cycle for $\Lambda < \Lambda_h$ and no recurrent behavior for $\Lambda > \Lambda_h$, again explaining the results in Fig. 11.

Bogdanov–Takens Bifurcation of Trivial Solution

Analyzing a similar type of system, Namachchivaya and Malhotra (1992) observed an interesting phenomenon: a homoclinic bifurcation near the Bogdanov–Takens bifurcation point, which is the intersection of two codimension-one bifurcation varieties, the static bifurcation and the Hopf bifurcation. The corresponding linear operator has a double-zero eigenvalue.

For the case of a simply supported panel in a supersonic stream, the critical values $\Lambda_{cr} = 679.2$ and $F_{cr} = 519.6$ at point c in Fig. 4 are obtained by satisfying the two conditions $r_3 = 0$ and $r_4 = 0$, where r_3 and r_4 are defined in (43c,d). The corresponding linear operator L_{cr} has the Jordan form

$$\hat{J} = P^{-1}L_{cr}P = \begin{bmatrix} 0 & 1 & 0 & 0 \\ 0 & 0 & 0 & 0 \\ 0 & 0 & -(\mu_1 + \mu_2) & 1 \\ 0 & 0 & 0 & -(\mu_1 + \mu_2) \end{bmatrix}. \quad (51)$$

Center manifold theory (Carr, 1981) can then be applied near this nonhyperbolic fixed point to reduce the fourth-order system to a second-order equation defined on a two-dimensional center manifold. Substituting $\underline{x} = P\underline{y}$ into Eq. (39) and premultiplying by P^{-1} yields

$$\underline{y}' = \hat{J}\underline{y} + P^{-1}(L - L_{cr})P\underline{y} + P^{-1}\underline{N}(P\underline{y}). \quad (52)$$

The center manifold of the decoupled system has the form

$$y_3 = h_1(y_1, y_2, \Lambda, F) \quad (53a)$$

$$y_4 = h_2(y_1, y_2, \Lambda, F) \quad (53b)$$

Because the nonlinearities are cubic, this center manifold can be approximated by cubic functions. Therefore, the dynamics of the center manifold is governed by equations of the following form:

$$\begin{bmatrix} y_1' \\ y_2' \end{bmatrix} = J \begin{bmatrix} y_1 \\ y_2 \end{bmatrix} + E(\Lambda, F) \begin{bmatrix} y_1 \\ y_2 \end{bmatrix} + \underline{\tilde{N}}(y_1, y_2) \quad (54)$$

where

$$J = \begin{bmatrix} 0 & 1 \\ 0 & 0 \end{bmatrix},$$
$$\underline{\tilde{N}} = \varepsilon \begin{bmatrix} \alpha_1 y_1^3 + \alpha_2 y_1^2 y_2 + \alpha_3 y_1 y_2^2 + \alpha_4 y_2^3 \\ \alpha_5 y_1^3 + \alpha_6 y_1^2 y_2 + \alpha_7 y_1 y_2^2 + \alpha_8 y_2^3 \end{bmatrix}, \quad (55)$$

and E is a 2×2 submatrix of $P^{-1}(L - L_{cr})P$. Letting

$$B = J + E = \begin{bmatrix} b_{11} & b_{12} \\ b_{21} & b_{22} \end{bmatrix}, \quad (56)$$

$$\det B = b_{11}b_{22} - b_{21}b_{12}, \quad \text{and} \quad \operatorname{tr} B = b_{11} + b_{22}$$

one can introduce the transformation

$$\begin{bmatrix} \eta_1 \\ \eta_2 \end{bmatrix} = \begin{bmatrix} 1 & 0 \\ b_{11} & b_{12} \end{bmatrix} \begin{bmatrix} y_1 \\ y_2 \end{bmatrix} \quad (57)$$

to transform Eq. (54) into the following form:

$$\begin{bmatrix} \eta_1' \\ \eta_2' \end{bmatrix} = \begin{bmatrix} 0 & 1 \\ -\det B & \operatorname{tr} B \end{bmatrix} \begin{bmatrix} \eta_1 \\ \eta_2 \end{bmatrix} + \underline{\tilde{N}}(\eta_1, \eta_2). \quad (58)$$

Again, one can use the method of normal forms to simplify Eq. (58).

For the time being, one can drop $\det B$ and $\operatorname{tr} B$ because they are sufficiently small. Then, we consider

$$\underline{\eta}' = J\underline{\eta} + \underline{\tilde{N}}(\underline{\eta}) \quad (59)$$

and introduce a near-identity transformation as well as the normal form

$$\underline{\eta} = \underline{\xi} + \varepsilon \underline{h}(\underline{\xi}) + \cdots \quad (60a)$$
$$\underline{\xi}' = J\underline{\xi} + \varepsilon \underline{g}(\underline{\xi}) + \cdots. \quad (60b)$$

Substituting Eqs. (60) into (59) yields

$$\begin{bmatrix} g_1 \\ g_2 \end{bmatrix} + \begin{bmatrix} \dfrac{\partial h_1}{\partial \xi_1} & \dfrac{\partial h_1}{\partial \xi_2} \\ \dfrac{\partial h_2}{\partial \xi_1} & \dfrac{\partial h_2}{\partial \xi_2} \end{bmatrix} \begin{bmatrix} 0 & 1 \\ 0 & 0 \end{bmatrix} \begin{bmatrix} \xi_1 \\ \xi_2 \end{bmatrix} - \begin{bmatrix} 0 & 1 \\ 0 & 0 \end{bmatrix} \begin{bmatrix} h_1 \\ h_2 \end{bmatrix} = \begin{bmatrix} \alpha_1 \xi_1^3 + \alpha_2 \xi_1^2 \xi_2 + \alpha_3 \xi_1 \xi_2^2 + \alpha_4 \xi_2^3 \\ \alpha_5 \xi_1^3 + \alpha_6 \xi_1^2 \xi_2 + \alpha_7 \xi_1 \xi_2^2 + \alpha_8 \xi_2^3 \end{bmatrix}. \quad (61)$$

The form of the nonlinearity suggests seeking the g_i and h_i in the following forms:

$$h_1 = \Gamma_1 \xi_1^3 + \Gamma_2 \xi_1^2 \xi_2 + \Gamma_3 \xi_1 \xi_2^2 + \Gamma_4 \xi_2^3 \quad (62a)$$
$$h_2 = \Gamma_5 \xi_1^3 + \Gamma_6 \xi_1^2 \xi_2 + \Gamma_7 \xi_1 \xi_2^2 + \Gamma_8 \xi_2^3 \quad (62b)$$
$$g_1 = \Lambda_1 \xi_1^3 + \Lambda_2 \xi_1^2 \xi_2 + \Lambda_3 \xi_1 \xi_2^2 + \Lambda_4 \xi_2^3 \quad (62c)$$
$$g_2 = \Lambda_5 \xi_1^3 + \Lambda_6 \xi_1^2 \xi_2 + \Lambda_7 \xi_1 \xi_2^2 + \Lambda_8 \xi_2^3. \quad (62d)$$

Substituting Eq. (62) into (61) yields

$$\begin{aligned} &\Lambda_1 \xi_1^3 + \Lambda_2 \xi_1^2 \xi_2 + \Lambda_3 \xi_1 \xi_2^2 + \Lambda_4 \xi_2^3 \\ &\quad + \xi_2(3\Gamma_1 \xi_1^2 + 2\Gamma_2 \xi_1 \xi_2 + \Gamma_3 \xi_2^2) \\ &\quad - (\Gamma_5 \xi_1^3 + \Gamma_6 \xi_1^2 \xi_2 + \Gamma_7 \xi_1 \xi_2^2 + \Gamma_8 \xi_2^3) \\ &\quad = \alpha_1 \xi_1^3 + \alpha_2 \xi_1^2 \xi_2 + \alpha_3 \xi_1 \xi_2^2 + \alpha_4 \xi_2^3 \quad (63) \\ &\Lambda_5 \xi_1^3 + \Lambda_6 \xi_1^2 \xi_2 + \Lambda_7 \xi_1 \xi_2^2 + \Lambda_8 \xi_2^3 \\ &\quad + \xi_2(3\Gamma_5 \xi_1^2 + 2\Gamma_6 \xi_1 \xi_2 + \Gamma_7 \xi_2^2) \\ &\quad = \alpha_5 \xi_1^3 + \alpha_6 \xi_1^2 \xi_2 + \alpha_7 \xi_1 \xi_2^2 + \alpha_8 \xi_2^3. \quad (64) \end{aligned}$$

Equating the coefficients of ξ_1^3, $\xi_1^2\xi_2$, $\xi_1\xi_2^2$, and ξ_2^3 on both sides of Eqs. (63) and (64), one has

$$C\underline{\Gamma} = \underline{\alpha} - \underline{\Lambda} \quad (65)$$

where

$$C = \begin{bmatrix} 0 & 0 & 0 & 0 & -1 & 0 & 0 & 0 \\ 3 & 0 & 0 & 0 & 0 & -1 & 0 & 0 \\ 0 & 2 & 0 & 0 & 0 & 0 & -1 & 0 \\ 0 & 0 & 1 & 0 & 0 & 0 & 0 & -1 \\ 0 & 0 & 0 & 0 & 0 & 0 & 0 & 0 \\ 0 & 0 & 0 & 0 & 3 & 0 & 0 & 0 \\ 0 & 0 & 0 & 0 & 0 & 2 & 0 & 0 \\ 0 & 0 & 0 & 0 & 0 & 0 & 1 & 0 \end{bmatrix}. \quad (66)$$

Here $\underline{\Gamma}$, $\underline{\alpha}$, and $\underline{\Lambda}$ are column vectors having the components Γ_m, α_m, and Λ_m, respectively.

Because C is a singular matrix, the system (65) has a solution if and only if $\underline{\alpha} - \underline{\Lambda}$ is orthogonal to every nontrivial solution $\underline{u}$ of the adjoint homogeneous problem; that is, $C^T\underline{u} = \underline{0}$. One then has

$$\underline{u} = (0, 0, 0, 0, 1, 0, 0, 0)^T \quad \text{and} \quad (3, 0, 0, 0, 0, 1, 0, 0)^T$$

and accordingly obtains

$$\Lambda_5 = \alpha_5 \tag{67a}$$

$$3\Lambda_1 + \Lambda_6 = 3\alpha_1 + \alpha_6. \tag{67b}$$

One can solve Eq. (65) for $\underline{\Gamma}$ for all values of the α_m, and hence Λ_k, $k = 2, 3, 4, 7$, and 8 can be set equal to zero. If one has $\Lambda_1 = 0$ and accounts for the two unfolding parameters, $\beta_1 = -\det B$ and $\beta_2 = \text{tr } B$, the corresponding truncated normal form of Eq. (58) can be expressed as

$$\xi_1' = \xi_2 \tag{68a}$$

$$\xi_2' = \beta_1\xi_1 + \beta_2\xi_2 + \gamma_1\xi_1^3 + \gamma_2\xi_1^2\xi_2 \tag{68b}$$

where

$$\beta_1 = -0.009(\Lambda - \Lambda_{cr}) + 0.023(F - F_{cr}) \tag{69a}$$

$$\beta_2 = 0.012(\Lambda - \Lambda_{cr}) - 0.019(F - F_{cr}) \tag{69b}$$

$$\gamma_1 = \varepsilon\alpha_5 = 0.028 \tag{69c}$$

$$\gamma_2 = \varepsilon(3\alpha_1 + \alpha_6) = -0.097. \tag{69d}$$

The global bifurcation behavior arising from this local codimension–two bifurcation is well known (Guckenheimer and Holmes, 1983).

SUMMARY

The nonlinear response of 2-DOF systems with one-to-one internal and principal parametric resonances is obtained by the method of normal forms. The same technique along with center manifold theory is used to analyze the bifurcation behavior near the nonhyperbolic fixed points. Because the stability of hyperbolic fixed points or periodic solutions can be studied by the corresponding eigenvalues or Floquet multipliers, respectively, one would then obtain a clearer picture of the dynamic behavior from the bifurcation diagram. In the case of a simply supported panel in a supersonic stream, qualitative changes can be predicted when either the forcing amplitude or the aerodynamic pressure is varied across a bifurcation curve. It is shown that the trivial solutions can lose stability through three types of bifurcations: supercritical and subcritical pitchfork bifurcations, supercritical Hopf bifurcations, and Bogdanov–Takens bifurcations. The stability of the equilibrium and periodic solutions are investigated. The Shilnikov theorem is used to explain the numerical results obtained near the formation of an orbit homoclinic to a saddle-focus fixed point.

This work was supported by the Air Force Office of Scientific Research under Grant No. F49620-92-J-0197.

REFERENCES

Asmis, K. G., and Tso, W. K., 1972, "Combination Resonance in a Nonlinear Two-Degree-of-Freedom System," *Journal of Applied Mechanics*, Vol. E39, pp. 832–834.

Asrar, W., 1991, "Two-Degree-of-Freedom Systems with Quadratic Non-Linearities Subjected to Parametric and Self Excitation," *Journal of Sound and Vibration*, Vol. 150, pp. 447–456.

Carr, J., 1981, *Applications of Center Manifold Theory*, *Applied Mathematical Sciences*, Vol. 35, Springer-Verlag, New York.

Ciliberto, S., and Gollub, J. P., 1985, "Chaotic Mode Competition in Parametrically Forced Surface Waves," *Journal of Fluid Mechanics*, Vol. 158, pp. 381–398.

Dowell, E. H., 1975, *Aeroelasticity of Plates and Shells*, Noordhoff, Leyden.

Dowell, E. H., and Ilgamov, M., 1988, *Studies in Nonlinear Aeroelasticity*, Springer–Verlag, New York.

Evan–Iwanowski, R. M., 1976, *Resonance Oscillations in Mechanical Systems*, Elsevier, New York.

Feng, Z. C., and Sethna, P. R., 1989, "Symmetry-Breaking Bifurcations in Resonant Surface Waves," *Journal of Fluid Mechanics*, Vol. 199, pp. 495–518.

Fu, F. C. L., and Nemat–Nasser, S., 1972a, "On the Stability of Steady-State Response of Certain Nonlinear Dynamic Systems Subjected to Harmonic Excitations," *Ingenieur-Archiv*, Vol. 41, pp. 407–420.

Fu, F. C. L., and Nemat–Nasser, S., 1972b, "Stability of Solution of Systems of Linear Differential Equations with Harmonic Coefficients," *AIAA J.*, Vol. 10, pp. 30–36.

Gu, X. M., and Sethna, P. R., 1987, "Resonant Surface Waves and Chaotic Phenomena," *Journal of Fluid Mechanics*, Vol. 183, pp. 543–565.

Guckenheimer, J., and Holmes, P. J., 1983, *Dynamical Systems and Bifurcations of Vector Fields*, Springer–Verlag, New York.

Holmes, P. J., 1986, "Chaotic Motions in a Weakly Nonlinear Model for Surface Waves," *Journal of Fluid Mechanics*, Vol. 162, pp. 365–388.

Ibrahim, R. A., 1985, *Parametric Random Vibration*, Wiley, New York.

Ibrahim, R. A., and Barr, A. D. S., 1975, "Autoparametric Resonance in a Structure Containing a Liquid. Part I: Two Mode Interaction," *Journal of Sound and Vibration*, Vol. 42, pp. 159–179.

Meron, E., and Procaccia, I., 1986, "Low-Dimensional Chaos in Surface Waves: Theoretical Analysis of an Experiment," *Physical Review*, Vol. A34, pp. 3221–3237.

Miles, J. W., 1984, "Nonlinear Faraday Resonance," *Journal of Fluid Mechanics*, Vol. 146, pp. 285–302.

Miles, J. W., 1985, "Parametric Excitation of an Internally Resonant Double Pendulum," *Journal of Applied Mathematics and Physics (ZAMP)*, Vol. 36, pp. 337–345.

Namachchivaya, N. S., and Malhotra, N., 1992, "Parametrically Excited Hopf Bifurcation with Non-Semisimple 1:1 Resonance," *Nonlinear Vibrations*, DE-Vol. 50/AMD-Vol. 144, pp. 29–46.

Nayfeh, A. H., 1983a, "Parametrically Excited Multidegree-of-Freedom Systems with Repeated Frequencies," *Journal of Sound and Vibration*, Vol. 88, pp. 145–150.

Nayfeh, A. H., 1983b, "The Response of Multidegree-of-Freedom Systems with Quadratic Nonlinearities to a Harmonic Parametric Resonance," *Journal of Sound and Vibration*, Vol. 90, pp. 237–244.

Nayfeh, A. H., 1983c, "The Response of a Two-Degree-of-Freedom Systems with Quadratic Nonlinearities to a Parametric Excitation," *Journal of Sound and Vibration*, Vol. 88, pp. 547–557.

Nayfeh, A. H., 1987a, "Parametric Excitation of Two Internally Resonant Oscillators," *Journal of Sound and Vibration*, Vol. 119, pp. 95–109.

Nayfeh, A. H., 1987b, "Surface Waves in Closed Basins under Parametric and Internal Resonances," *Physics of Fluids*, Vol. 30, pp. 2976–2982.

Nayfeh, A. H., 1993, *Method of Normal Forms*, Wiley, New York.

Nayfeh, A. H., and Balachandran, B., 1989, "Modal Interactions in Dynamical and Structural Systems," *Applied Mechanics Reviews*, Vol. 42, pp. 175–201.

Nayfeh, A. H., and Balachandran, B., 1994, *Applied Nonlinear Dynamics*, Wiley, New York.

Nayfeh, A. H., and Balachandran, B., 1995, *Nonlinear Interactions*, Wiley, New York, to appear.

Nayfeh, A. H., and Mook, D. T., 1979, *Nonlinear Oscillations*, Wiley, New York.

Nayfeh, A. H., and Nayfeh, J. F., 1990, "Surface Waves in Closed Basins Under Principal and Autoparametric Resonances," *Physics of Fluids*, Vol. A2, pp. 1635–1648.

Nayfeh, A. H., and Pai, P. F., 1989, "Non-Linear Non-Planar Parametric Responses of an Inextensional Beam," *International Journal of Non-Linear Mechanics*, Vol. 24, pp. 139–158.

Nayfeh, A. H., and Zavodney, L. D., 1986, "The Response of Two-Degree-of-Freedom Systems with Quadratic Non-Linearities to a Combination Parametric Resonance," *Journal of Sound and Vibration*, Vol. 107, pp. 329–350.

Schmidt, G., and Tondl, A., 1986, *Nonlinear Vibrations*, Akademie–Verlag, Berlin.

Shilnikov, L. P., 1970, "A Contribution to the Problem of the Structure of an Extended Neighborhood of a Rough Equilibrium State of Saddle-Focus Type," *Mathematics of the USSR-Sbornik*, Vol. 10, pp. 91–102.

Simonelli, F., and Gollub, J. P., 1989, "Surface Wave Mode Interactions: Effects of Symmetry and Degeneracy," *Journal of Fluid Mechanics*, Vol. 199, pp. 471–494.

Streit, D. A., Bajaj, A. K., and Krousgrill, C. M., 1988, "Combination Parametric Resonance Leading to Periodic and Chaotic Response in Two-Degree-of-Freedom Systems with Quadratic Nonlinearities," *Journal of Sound and Vibration*, Vol. 124, pp. 297–314.

Tezak, E. G., Mook, D. T., and Nayfeh, A. H., 1978, "Nonlinear Analysis of the Lateral Response of Columns to Periodic Loads," *Journal of Mechanical Design*, Vol. 100, pp. 651–659.

Tezak, E. G., Nayfeh, A. H., and Mook, D. T., 1982, "Parametrically Excited Nonlinear Multidegree-of-Freedom Systems with Repeated Natural Frequencies," *Journal of Sound and Vibration*, Vol. 85, pp. 459–472.

Tso, W. K., and Asmis, K. G., 1974, "Multiple Parametric Resonance in a Non-Linear Two Degree of Freedom System," *International Journal of Non-Linear Mechanics*, Vol. 9, pp. 269–277.